Clinical and Experimental Medicine (2019) 19:201–210
https://doi.org/10.1007/s10238-018-0541-2

ORIGINAL ARTICLE

PLX9486 shows anti-tumor efficacy in patient-derived, tyrosine kinase inhibitor-resistant KIT-mutant xenograft models of gastrointestinal stromal tumors

Yemarshet K. Gebreyohannes[1,2] · Elizabeth A. Burton[3] · Agnieszka Wozniak[1,2] · Bernice Matusow[3] · Gaston Habets[3] · Jasmien Wellens[1,2] · Jasmien Cornillie[1,2] · Jack Lin[3] · Marika Nespi[3] · Guoxian Wu[3] · Chao Zhang[3] · Gideon Bollag[3] · Maria Debiec-Rychter[4] · Raf Sciot[5] · Patrick Schöffski[1,2]

Received: 5 July 2018 / Accepted: 26 November 2018 / Published online: 6 December 2018

Abstract

The purpose of the present study was to investigate the in vitro and in vivo activity of PLX9486, a tyrosine kinase inhibitor (TKI) targeting both primary *KIT* exon 9 and 11 and secondary exon 17 and 18 mutations in gastrointestinal stromal tumors (GISTs). Imatinib, a potent inhibitor of mutated KIT, has revolutionized the clinical management of advanced, metastatic GIST. However, secondary resistance develops mainly through acquired mutations in *KIT* exons 13/14 or exons 17/18. Second-line sunitinib potently inhibits *KIT* exon 13/14 mutants but is ineffective against exon 17 mutations. In our study, PLX9486 demonstrated in vitro nanomolar potency in inhibiting the growth and KIT phosphorylation of engineered BaF3 cells transformed with *KIT* exon 17 mutations (p.D816V) and with the double *KIT* exon 11/17 mutations (p.V560G/D816V). The in vivo efficacy of PLX9486 was evaluated using two imatinib-resistant GIST patient-derived xenograft (PDX) models. In UZLX-GIST9 (*KIT:* p.P577del;W557LfsX5;D820G), PLX9486 100 mg/kg/day resulted in significant inhibition of proliferation. Pharmacodynamic analysis showed a pronounced reduction in mitogen-activated protein kinase (MAPK) activation and other downstream effects of the KIT signaling pathway but no significant effect on KIT Y703 and Y719 phosphorylation. Similarly, in MRL-GIST1 (*KIT*: p.W557_K558del;Y823D) PLX9486 treatment led to significant tumor regression and strong inhibition of MAPK activation. Interestingly, the inhibitory effect on MAPK activation was evident even after a single dose of PLX9486. In conclusion, PLX9486 showed anti-tumor efficacy in patient-derived imatinib-resistant GIST xenograft models, mainly through inhibition of KIT signaling. These preclinical efficacy data encourage further testing of PLX9486 in the clinical setting.

Keywords Gastrointestinal stromal tumors · PLX9486 · Tyrosine kinase inhibitor · Resistance

Introduction

Gastrointestinal stromal tumors (GISTs) are rare mesenchymal tumors arising in the wall of the digestive tract [1]. The vast majority of these tumors are driven by activating mutations in genes encoding the KIT receptor or the platelet-derived growth factor receptor alpha (PDGFRA) [2]. These mutations result in the constitutive activation of the respective receptor tyrosine kinases (RTKs) and downstream signaling cascades, including phosphatidylinositol-3-kinase (PI3K)/AKT/mammalian target of rapamycin (mTOR) and RAS/RAF/mitogen-activated protein kinase (MAPK) pathways. These changes ultimately converge and result in uncontrolled GIST cell proliferation and survival [2].

Electronic supplementary material The online version of this article (https://doi.org/10.1007/s10238-018-0541-2) contains supplementary material, which is available to authorized users.

✉ Agnieszka Wozniak
agnieszka.wozniak@kuleuven.be

1 Laboratory of Experimental Oncology, Department of Oncology, KU Leuven, Herestraat 49 Post 815, 3000 Leuven, Belgium

2 Department of General Medical Oncology, Leuven Cancer Institute, University Hospitals Leuven, Leuven, Belgium

3 Plexxikon Inc., Berkeley, CA, USA

4 Department of Human Genetics, KU Leuven and University Hospitals, Leuven, Belgium

5 Department of Pathology, KU Leuven and University Hospitals, Leuven, Belgium

More than 50% of primary, localized and resectable GIST can be cured by surgery alone [3]. However, approximately 25% of patients present with metastatic disease at diagnosis, and about 40% of patients who had initial gross macroscopic surgical removal experience recurrence during the further course of the disease [2]. Recurrent or metastatic GISTs are treated using tyrosine kinase inhibitors (TKIs) such as imatinib, which is a potent antagonist of activated KIT and achieves a disease control rate of 75–85% [1]. The outcome of TKI treatment is strongly influenced by the type of oncogenic *KIT* mutation [4]. Higher response rates as well as longer median overall survival times have been reported in GIST patients with *KIT* exon 11 mutations, the most common primary mutation, as compared with *KIT* exon 9 mutated GIST, which requires a higher dose of imatinib [4]. Nevertheless, the majority of GIST patients treated with imatinib develop resistance over time and ultimately progress, mainly due to the acquisition of secondary mutations in the KIT receptor kinase domain, most commonly in regions encoded by exons 13/14 and 17/18 [5]. Sunitinib and regorafenib, which have activity against imatinib-resistant GIST, are used as second- and third-line treatments after imatinib failure [6, 7]. Unfortunately, due to the heterogeneity of resistant clones or other factors, the response duration tends to be shorter with every subsequent treatment. Sunitinib is active against *KIT* exon 13 and 14 alterations (e.g., p.V654A or p.T670I) because its binding is unencumbered by the mutation. However, secondary mutations in the activation loop (A-loop) of the receptor, encoded by *KIT* exons 17 and 18, are resistant to both imatinib and sunitinib [5, 8]. Regorafenib is the only approved agent for the treatment of GIST after failure of both imatinib and sunitinib. Although it has demonstrated activity against some mutations in the A-loop, the clinical benefit from regorafenib is rather limited by its inability to inhibit the p.D816V mutation, and disease progression typically occurs after a median treatment duration of less than a year [7, 9, 10]. Therefore, to address GIST mutation heterogeneity more effectively, there is a need to develop new compounds that can block the entire spectrum of *KIT* A-loop mutations.

PLX9486 (Plexxikon) is a selective TKI, targeting mutated *KIT* and demonstrating potent activity in vitro against primary exon 9 and 11 mutations, as well as secondary A-loop mutations located in exons 17 and 18 [11]. In the current study, we describe the in vitro efficacy of PLX9486 using BaF3 cell assays and the in vivo activity of PLX9486 in two imatinib-resistant patient-derived xenograft (PDX) models with double *KIT* exon 11 and 17 mutations.

Materials and methods

Cell culture, BaF3 *KIT* inhibition assay

BaF3 is a murine pro-B cell line that depends on interleukin 3 (IL3) for growth and survival which can be complemented by introducing exogenous activated kinases [12]. BaF3 parental cells (DSMZ #ACC300) were cultured in RPMI in the presence of 10% fetal bovine serum, 1% non-essential amino acids, 1% L-glutamine and 1% penicillin–streptomycin (all Thermo Fisher) in the presence of IL3. *KIT* expression construct was generated by cloning the full-length, wild-type human KIT *(KIT-WT)* sequence into the pCI-Neo mammalian expression vector (Promega Corporation) allowing selection of clones with geneticin (G418; Life Technologies). Expression constructs with *KIT* p.D816V and the double mutant *KIT* p.V560G/D816V were created with site-directed mutagenesis (Quikchange, Agilent). BaF3 parental cells were stably transfected with the expression plasmids by electroporation (Bio-Rad), and G418-resistant clones were isolated by limiting dilution and tested for IL-3 independence (for the *KIT* p.D816V and *KIT* p.V560G/D816V clones) or dependence on stem cell factor (SCF) (for the *KIT-WT* clone). For compound testing of growth inhibition, two replicate 96-well plates (Corning) were plated at a density of 10,000 cells per well. The cells were plated in 50 µL volume of cell culture medium without IL3 the day before incubation with eight-point dilution ranges of either test compound, PLX9486 or imatinib. Dilution series of test compounds were made in 100% DMSO and then mixed 1/250 (*v*/*v*) in growth medium of which 50 µL was added per well, resulting in final concentration ranges of 10 µM to 4.6 nM or 1 µM to 0.46 nM. The high or low concentration range was chosen to get a most accurate determination of the compounds IC50 in a particular cell line and assay condition. The compound-treated cells were incubated for 3 days at 37 °C, and relative proliferation was measured by addition of CellTiter-Glo® Luminescent Cell Viability Assay Reagent (Promega) and measurement of luminescence. Luminescence values were normalized to 0.2% DMSO-treated control wells. Compound inhibition tests were repeated over multiple weeks with new compound preparations and cell cultures. PLX9486 was tested in BaF3 *KIT-WT* in eight independent experiments, in BaF3 *KIT* p.D816V in seven and in BaF3 *KIT* p.V560G/D816V in three experiments.

For compound inhibition of KIT phosphorylation, 100,000 cells were plated in 50 µL per well without IL3 in 96-well poly-D-lysine-coated plates and left to adhere for 1 h. Dilution series of test compounds were subsequently added to the cells as described for testing of growth inhibition. Cells were incubated at 37 °C for 1 h after which

medium was removed and cells were lysed on ice for 5 min (lysis buffer (1×) Perkin Elmer). Total KIT phosphorylation was detected by AlphaScreen® technology (Perkin Elmer) by mixing equal volumes (5 µL each) of lysate, PY20 acceptor beads (Perkin Elmer), biotinylated antihuman KIT antibody (R&D Systems) and streptavidin-coated donor beads (Perkin Elmer) to a 384-well AlphaPlate (Perkin Elmer). After 2-h incubation at room temperature, plates were read using an Alpha-signal-enabled plate reader (Perkin Elmer). Eight DMSO-only positive and eight no KIT capture antibody-negative control wells were included in each plate and used for signal normalization and assay controls.

GIST xenografts

The in vivo efficacy of PLX9486 was assessed using two GIST PDX models UZLX-GIST9 (*KIT*: p.P577del;W557LfsX5;D820G) [13] and MRL-GIST1 (2007031011; Pt ID 152499) (*KIT:* p.W557_K558del;Y823D) [14]. Both models maintained stable morphological and immunohistochemical features as well as the presence of *KIT* mutations identical to the original patient sample and earlier passages [13, 14]. The UZLX-GIST9 study was performed in the Laboratory of Experimental Oncology, KU Leuven, Belgium, and the MRL-GIST1 study was carried out under contract at Molecular Response Laboratory (MRL), San Diego, USA, currently CrownBio. Both in vivo experiments were approved by respective ethics board and conducted according to their rules and national regulations.

Compounds, reagents and experimental design

For both experiments, PLX9486, imatinib, 1-methyl-2-pyrrolidone (NMP) solvent and the diluent (PEG400/tocopherol polyethylene glycol succinate/poloxamer 407/water, 40:5:5:50 *v*/*v*) were provided by Plexxikon. The stock solution of imatinib and PLX9486 (200 mg/ml each) was prepared in NMP every 10 days. The final dosing solutions were formulated daily by diluting the stock solutions with the diluent (1 in 10 *v*/*v*). Mice were dosed once a day, using an oral gavage. Using historical data from various experiments, the coefficient of variation for proliferation [measured by the mitotic index or phospho-histone H3 (pHH3) count] was estimated in the range 0.5–0.6. Based on a two-sample two-sided *t* test (with alpha equal to 0.05) for a mean ratio, 11–15 tumors per group (6–8 experimental animals, transplanted bilaterally) were needed to detect a 50% reduction in proliferation (mitotic count) with at least 80% power. UZLX-GIST9 mice ($n=23$, transplanted bilaterally) were treated with vehicle (NMP/diluent; 1:10 *v*/*v*; $n=7$), imatinib (100 mg/kg/qd; $n=7$) or PLX9486 (100 mg/kg/qd; $n=9$) for 28 days. In the second experiment, mice carrying a single MRL-GIST1 tumor were treated with vehicle ($n=6$) or PLX9486 (100 mg/kg/qd, $n=13$) for 22 days. On the last day of the latter experiment, two of the vehicle control mice were administered with a single dose of PLX9486, two hours prior to termination, to assess early effects of the compound. For both experiments, the drug efficacy was assessed by three-dimensional tumor measurements using an electronic caliper three times per week. The body weight and general well-being of mice were followed up daily during the treatment period. Tumor samples collected on the last day of experiments were analyzed by histopathology. Western blotting (WB) was performed to evaluate KIT pathway signaling in the UZLX-GIST9 tumors.

Immunohistochemistry (IHC) and WB analysis were conducted using the following antibodies and reagents: phospho-KIT^{Y719}, phospho-KIT^{Y703}, phospho-AKT^{S473}, AKT, phospho-MAPK$^{T202/204}$, MAPK, phospho-S6$^{S240/244}$, S6, phospho-4E-translation initiation factor binding protein 1 (p-4EBP1^{S65}), 4EBP1, tubulin, pHH3 and horseradish peroxidase (HRP)-labeled anti-rabbit Signal Stain® Boost IHC detection (all from Cell Signaling Technologies), KIT (CD117), anti-rabbit Envision + System-HRP labeled polymer and 3′-diaminobenzidine-tetrahydrochloride (all from DAKO), discovered on GIST 1 (DOG1) (Leica Biosystems), Ki67 (Thermo Scientific), cleaved PARP (poly-ADP ribose polymerase) (Abcam), Western Lightning® Plus–ECL-enhanced chemiluminescence substrate reagents (Perkin Elmer).

Histopathology and western blotting

Paraffin sections (4 µm) were cut for hematoxylin and eosin (H&E) and IHC. KIT and DOG1 immunostainings were performed to confirm GIST diagnosis. Histologic response (HR) was evaluated by assessing the magnitude of necrosis, myxoid degeneration and/or fibrosis on H&E staining using the following previously described grading system: grade 1 (0–10%), grade 2 (> 10% and ≤ 50%), grade 3 (> 50% and ≤ 90%) and grade 4 (> 90%) [5]. Proliferative and apoptotic activities were evaluated as described before [15]. The level of MAPK phosphorylation was assessed on IHC by evaluating the intensity and percent of tumor area with positive pMAPK (Supplemental Table S1). In addition, for UZLX-GIST9, the status of KIT signaling was assessed by performing WB analysis as previously described [15].

Statistical analysis

Wilcoxon matched-pairs test (WMP) was used to compare the tumor volumes between baseline and the last day of the experiments. Mann–Whitney *U* test (MWU) was performed to compare results obtained with different treatments. A *p*

value < 0.05 was considered statistically significant. Statistica 13.0 (Dell Inc.) software was used for all statistical calculations.

Results

In vitro activity of PLX9486

The ability of PLX9486 to inhibit KIT catalytic activity in cells was evaluated using engineered BaF3 cells created by stable transfection of full-length DNA constructs containing *KIT-WT, KIT* p.D816V or *KIT* p.V560G/D816V. The BaF3 cell clones expressing the oncogenic *KIT* p.D816V and *KIT* p.V560G/D816V proliferated in the absence of IL3 at a rate similar to the parental BaF3 cells with IL3. The cells expressing the *KIT-WT* construct were shown to be dependent upon the KIT-ligand SCF for growth in the absence of IL3 and are sensitive to imatinib and PLX9486 inhibition (Table 1). BaF3 clones expressing *KIT* p.D816V or *KIT* p.V560G/D816V are essentially resistant to imatinib. PLX9486 is, however, a potent inhibitor of growth and KIT phosphorylation in the imatinib-sensitive and imatinib-resistant BaF3 cell lines (Table 1), with growth IC50 = 61 nM for *KIT*-WT and more potently against BaF3 *KIT* p.D816V (IC50 = 6.6 nM) and BaF3 *KIT* p.V560G/D816V (IC50 = 7.1 nM) (Fig. 1 and Table 1). Only the KIT-driven proliferation of the transfected BaF3 cells in the absence of IL3 is inhibited by PLX9486. The same cell clone tested in the presence of IL3 is essentially resistant to PLX9486 as illustrated by the IC50 shift from 7.1 nM to greater than 10,000 nM for BaF3 *KIT* p.V560G/D816V cells (Supplemental Fig. S1).

In vivo efficacy of PLX9486 in imatinib-resistant patient-derived xenograft models

The translation of in vitro cellular activity of PLX9486 on imatinib-resistant tumors with A-loop mutations was independently tested in two TKI-resistant human PDX models.

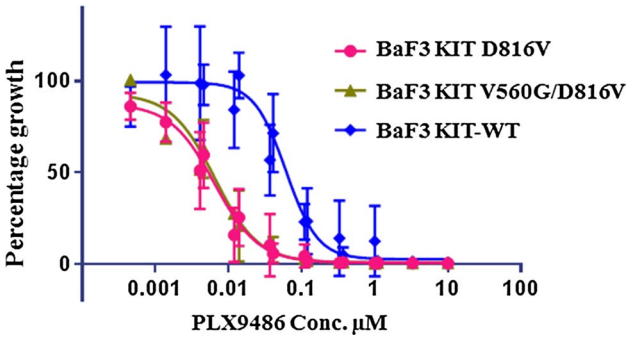

Fig. 1 Growth curves of BaF3 cells, treated with PLX9486, showing growth inhibition of cells with different *KIT* genotypes: *KIT* p.D816V (IC50 = 6.6 nM), *KIT* p.V560G/D816V (IC50 = 7.1 nM) or BaF3 *KIT-WT* stimulated with stem cell factor (IC50 = 61 nM). Data are shown as mean values ± standard error of the mean of relative cell growth

Tumor volume evaluation

Mice bearing bilateral tumors of UZLX-GIST9 were treated orally with vehicle, imatinib or PLX9486 (each 100 mg/kg/qd) for 28 days. On the last day of dosing (day 28), the mean tumor volumes increased by 125% from the baseline ($p = 0.002$, WMP) in the vehicle-treated group and by 79% in the imatinib-treated group ($p = 0.04$). In contrast, PLX9486 treatment led to a nearly complete tumor growth inhibition with only 14% increase in tumor volume compared to baseline ($p = 0.22$, WMP). The tumor volumes of PLX9486-treated animals were significantly smaller than those of the vehicle-treated group ($p < 0.001$, MWU) (Fig. 2a).

No significant body weight decrease (Supplemental Fig. S2) or treatment-related toxicity was observed in any of the treatment groups. One mouse in the PLX9486-treated group was sacrificed on day 22 for ethical reasons, because one of the tumors exceeded the acceptable volume, also hindering the mobility of the animal. Interestingly, histologic evaluation of the tumor revealed that although the tumor grew to 168% from baseline, the vast majority of cells (> 90% tumor area) were necrotic with only few zones containing viable cells (Fig. 2c).

Table 1 IC50 values for proliferation (growth) and total phospho-tyrosine KIT (pY-KIT) for imatinib and PLX9486 measured in BaF3 *KIT-WT*, *KIT* p.D816V and *KIT* pV560G/D816V cell clones

BaF3 cells KIT	WT	p.D816V		p.V560G/D816V	
IC50 [nM]	Growth	Growth	pY-KIT	Growth	pY-KIT
PLX9486	61 (47–78)	6.6 (4.6–9.6)	74 (< 4.6 and 74)	7.1 (4–12)	28 (11, 26, 77)
Imatinib	89 (71–110)	4100 (3200–5300)	> 10,000 $n = 3$	2800 (2200–3600)	> 10,000 $n = 3$

95% confidence interval (CI) is shown for individual observations with $n \leq 3$

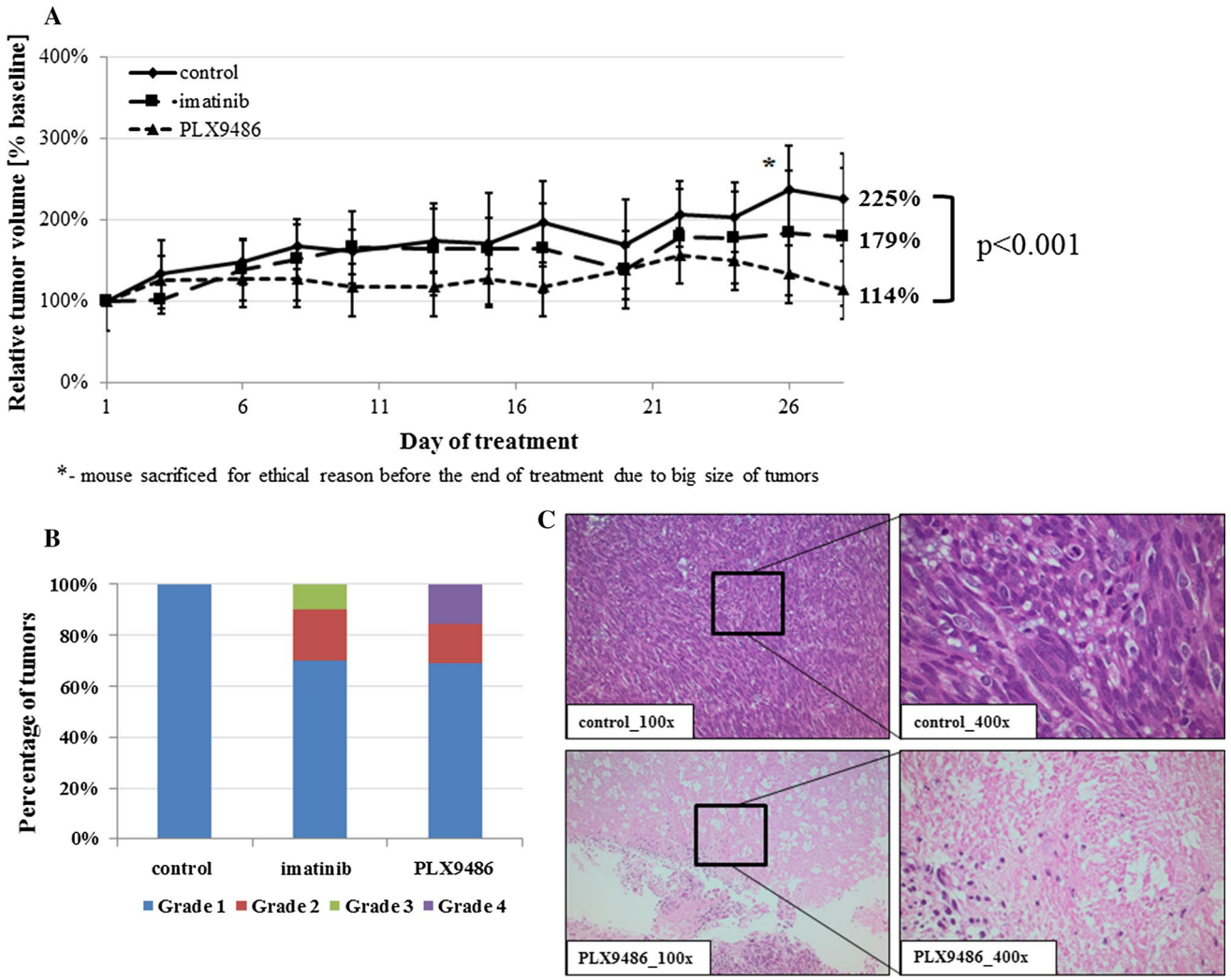

Fig. 2 Tumor volume evolution as percent of normalized baseline during 28 days of treatment in UZLX-GIST9 (**a**). Histologic response (HR) evaluated by assessing the magnitude of necrosis, myxoid degeneration and/or fibrosis on H&E staining (**b**). H&E images of control and PLX9486-treated tumors at 100-fold (×100) and 400-fold (×400) magnification showing features of histologic response (HR) (**c**)

A second in vivo efficacy study of PLX9486 was performed using the independently derived imatinib-resistant model MRL-GIST1. In this experiment, mice were treated orally with either the vehicle (control) or PLX9486 (100 mg/kg/qd) for 22 days. At the end of the treatment period, vehicle-treated tumors grew steadily to 306% of baseline. In contrast, the mean tumor volume in the PLX9486-treated tumors showed 34% regression (Fig. 3a). Of note, four mice in the control group were sacrificed on days 18 and 20 due to the growth of tumors exceeding the protocol limit (tumor volume > 2000 mm^3). The removal of the four control animals artificially increased the average body weight with two remaining larger animals. In the PLX9486 treatment group, no adverse effects were observed, and the body weight had only minor change (− 2.3%) from the start of treatment.

Histologic response

Treatment-related HR was assessed by evaluating the histologic features (necrosis or myxoid degeneration) in tumors, collected at the end of the in vivo experiment. In the UZLX-GIST9 model, minimal HR (grade 1) was observed in the tumors of the control group. PLX9486 caused HR grade 2 and 4 in 30% of tumors (Fig. 2b). Figure 2c shows an example of grade 4 necrosis observed in the PLX9486-treated tumors. In addition, two tumors (20%) in the imatinib group showed HR grade 2 and one tumor had grade 3.

In the MRL-GIST1, model treatment with PLX9486 for 22 days led to a grade 2 HR in 2 out of 3 tumors analyzed. The HR observed in this model was characterized by the induction of myxoid degeneration where viable cells were replaced by an amorphous collagen matrix with scattered

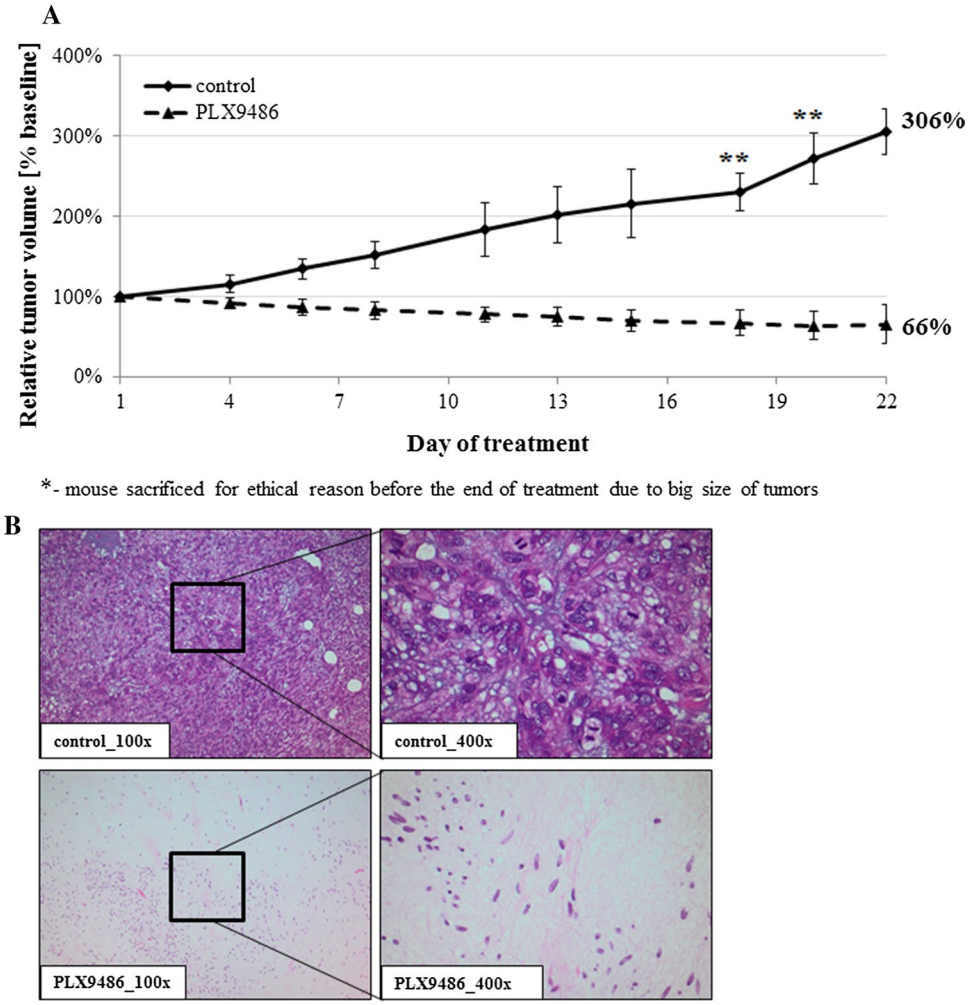

Fig. 3 Tumor volume evolution as percent of normalized baseline during 22 days of treatment in MRL-GIST1 (**a**), H&E images of control and PLX9486-treated tumors at 100-fold (×100) and 400-fold (×400) magnification showing features of histologic response (HR) in MRL-GIST1 (**b**)

cells (Fig. 3b). This phenomenon is characteristic of the response to imatinib in imatinib-responsive tumors in both preclinical and clinical settings [16].

Proliferative and apoptotic activity

The proliferative activity of the xenotransplants was assessed by counting the mitotic figures on H&E-stained slides and by pHH3 as well as Ki67 immunostainings. In UZLX-GIST9 model, vehicle-treated tumors showed a high mitotic activity [median 46 mitosis per 10 high power field (HPF)], which was not statistically different in imatinib-treated group (59.5 per 10 HPF). In contrast, PLX9486 treatment led to a dramatic decrease in the number of mitotic cells (0 per 10 HPF; $p < 0.001$, MWU in comparison with vehicle control) (Table 2). The effect of PLX9486 on proliferation was confirmed by pHH3 and Ki67 immunostainings (Table 2) No significant induction of apoptotic activity was observed in any of the end of treatment samples (Table 2).

Vehicle-treated MRL-GIST1 tumors were characterized by active proliferation; the average number of mitotic cells on H&E- and pHH3-positive cells per 10 HPF was 46.5 and 83, respectively. In contrast, the average number of mitotic cells on H&E, pHH3 and Ki67 stains was reduced to zero in PLX9486-treated tumors (Fig. 4). As in the UZLX-GIST9 model, no apoptotic activity was observed in the remaining MRL-GIST1 tumor samples after three weeks of PLX9486 treatment.

KIT signaling pathway evaluation

The status of KIT signaling under different treatments was compared using WB. In UZLX-GIST9 model, PLX9486 inhibited the activation of the downstream signaling cascade, as visualized by the reduced phosphorylation of AKT, MAPK, S6, and to some extent 4EBP1 (Fig. 5a), although no evident inhibition of KIT phosphorylation was observed in this model using two phospho-specific antibodies. The inhibitory effect on the MAPK activation was confirmed by IHC, where in most (> 70%) of vehicle- and imatinib-treated tumors the pMAPK staining was (very) strong. In contrast, PLX9486 treatment drastically reduced the level of pMAPK

Table 2 Histopathological assessment of the proliferative and apoptotic activity in tumors treated with imatinib and PLX9486

Treatment group	Proliferation			Apoptosis	
	Mitosis (H&E)	pHH3	Ki67	Apoptosis (H&E)	Cleaved PARP
Control	46.0 (n/a)	61.0 (n/a)	0.21 (n/a)	24.0 (n/a)	37.0 (n/a)
Imatinib	59.5 (=)	58.0 (=)	0.22 (=)	21.5 (=)	38.5 (=)
PLX9486	0 (↓↓↓)*	2.0 (↓31)*	0.01 (↓38)*	26 (=)	32 (=)

Values are presented as median and fold change in comparison with the control tumors (in brackets). Mann–Whitney *U* test was performed for statistical analysis, comparing result from the respective treatment arm with control group

H&E, hematoxylin and eosin staining; n/a, not applicable; PARP, poly-ADP ribose polymerase; pHH3, phospho-histone H3

↑, fold change increase; ↓, fold change decrease; ↓↓↓, > 100 fold change decrease; =, no significant difference in fold change; *$p < 0.005$ by MWU comparing result from the active treatment with control group

in the tumor tissue compared to the other treatment arms (Fig. 5b, c).

MAPK phosphorylation was also strongly reduced in the tumors of the MRL-GIST1 model after 22-day PLX9486 treatment (Fig. 4). At the end of the MRL-GIST1 study, two mice from the control group were treated with a single dose of PLX9486 and euthanized 2 h later. Interestingly, even this short-term treatment with PLX9486 caused a drastic decrease in MAPK phosphorylation in comparison with vehicle-treated tumors. The magnitude of MAPK phosphorylation inhibition after 2 h of PLX9486 treatment was comparable to that observed in the tumors treated for 22 days (Fig. 4). As expected, a single dose of PLX9486 did not influence the proliferation rate of tumor cells (Fig. 4).

Discussion

We present the activity of PLX9486, a potent and selective TKI, with efficacy in vitro using BaF3 cells and in vivo in two GIST imatinib-resistant PDX models. PLX9486 showed nanomolar potency for inhibition of both cell proliferation and total KIT tyrosine phosphorylation in the imatinib-resistant BaF3 *KIT* p.D816V and *KIT* p.V560G/D816V cell clones.

In vitro results were confirmed in vivo where PLX9486 showed significant anti-tumor activity in both PDX models tested, exhibited by strong inhibition of tumor size, histologic analyses of induction of HR and decreased proliferative activity. Interestingly, although both PDX models carry primary and secondary *KIT* exon 11 and 17 mutations and show similar resistance to imatinib [13, 14], the extent of anti-tumor effect of PLX9486 in the two models was different. While tumor regression was achieved in fast-growing MRL-GIST1 PDX, disease stabilization was observed in the slower-growing UZLX-GIST9 model. Technical reasons for this difference could include different growth properties of the xenografts, difference in the specific *KIT* genotype, or other molecular signatures of the two models.

The tumor stabilization in UZLX-GIST9 was accompanied by potent inhibition of proliferation as well as induction of histologic response. In the clinical setting, imatinib often causes tumor stabilization, often accompanied by dramatic histologic response [16]. In the early stage of treatment, increased tumor size (pseudoprogression) may occur due to osmotic changes related to rapid induction of intra-tumoral necrosis or myxoid degeneration, while tumor density and vascularization decrease [17]. In the UZLX-GIST9 model, two out of 13 tumors treated with PLX9486 exhibited grade 4 HR (the replacement of > 90% of tumor tissue with necrosis). While the tumor volume did not show regression, responses in mitotic index were strong and pathway signaling was inhibited. Similarly, we observed extensive necrosis in a tumor that had grown beyond the acceptable limit, leading to early sacrifice of that mouse from the PLX9486 treatment group (on day 22). We previously reported a similar observation in this model, where two-week treatment with the multi-targeted TKI cabozantinib led only to a delay in tumor growth, although the histologic evaluation revealed necrosis in 50% of the tumors [15].

Comparable to the imatinib-resistant BaF3 *KIT* p.D816V cell clones, PLX9486 treatment led to a substantial decrease in cell proliferation in both PDX models in vivo. In the UZLX-GIST9 model, this effect was superior to what was observed in imatinib-treated tumors. In contrast to the cell-based experiments, we could not detect inhibition of KIT phosphorylation by PLX9486 when analyzing total tumor lysates by WB using two phospho-specific antibodies. Nevertheless, a striking inhibitory effect on MAPK phosphorylation, downstream of the KIT receptor, was evident by IHC as well as WB analysis of ex-mouse tumors, and as early as 2 h after PLX9486 treatment in the MRL-GIST1 tumors. Several studies have recently shown that a direct inhibition of the MAPK pathway components led to a reduced GIST cell proliferation in vitro and in vivo [18, 19]. Ran

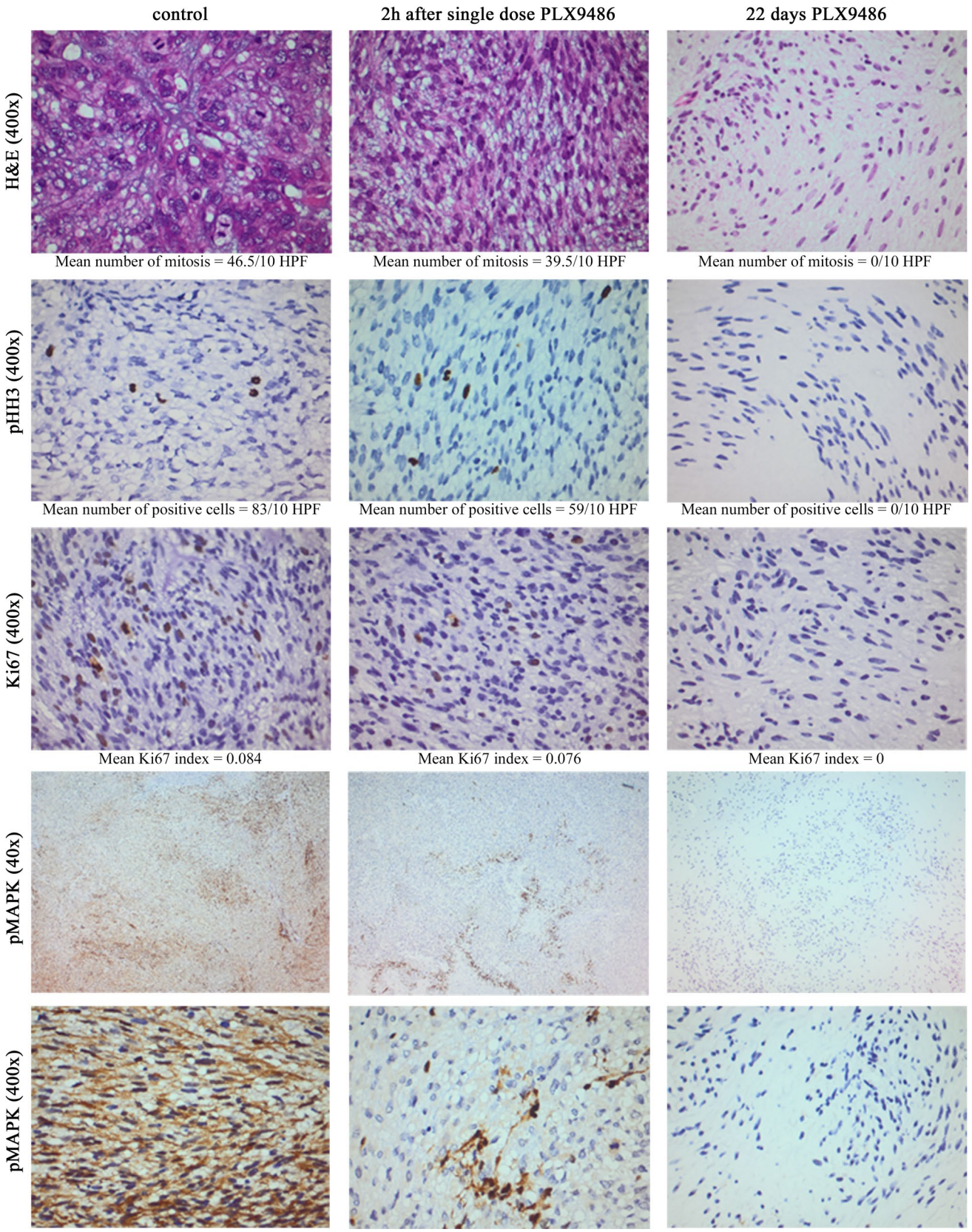

Fig. 4 Representative images of H&E and immunostaining of MRL-GIST1 tumors from control tumors 2 h (h) after single dose of PLX9486 and tumors treated with PLX9486 for 22 days

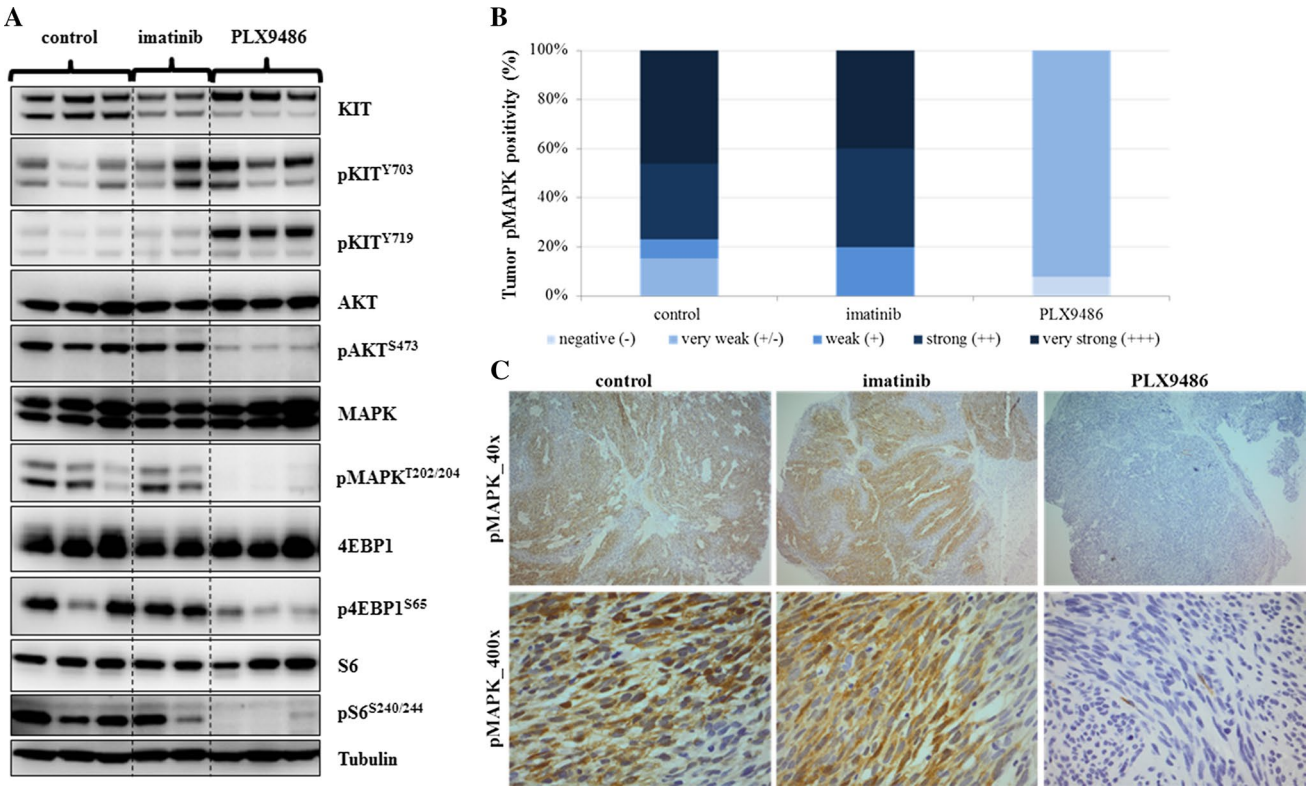

Fig. 5 Assessment of KIT signaling after 28 days of treatment in UZLX-GIST9. Western blotting analysis of KIT signaling pathway (**a**). Every single lane shows results from an independent tumor. Evaluation of pMAPK positivity per treatment group (**b**). Representative images of pMAPK at 40- and 400-fold magnification (**c**)

et al. demonstrated that the combination of imatinib and MEK162 (MEK inhibitor) resulted in a dramatic decrease in tumor volume in two GIST xenografts [18]. Moreover, the advantage of KIT and MAPK inhibition using combination therapy is also implicated in reversing resistance resulting from cross talk between different RTKs which signal mainly through the MAPK pathway [19]. Furthermore, we also saw an inhibition of PI3K pathway intermediates (AKT, 4EBP1 and S6 phosphorylation) by PLX9486, which could potentially add to the anti-proliferative effects of the compound tested.

PLX9486 treatment showed only a limited effect on apoptosis in both models. This could be due to the timing of the tumor harvest or related to dose as observed with a similar TKI, avapritinib (BLU-285) in our UZLX-GIST9, where a significant induction of apoptosis was only observed at the higher dose [20]. Secondly, UZLX-GIST9 is a model of aggressive GIST with a lot of spontaneous apoptotic activity even in the untreated tumors, which could be masking the treatment efficacy in terms of apoptosis induction [13]. Finally, there is evidence that in GIST the response to TKI (e.g., imatinib) is sustained by autophagy rather than apoptosis [21].

Currently, there are several promising novel therapeutic approaches being explored for the management of refractory GISTs in the preclinical and early clinical settings. These strategies investigate both novel targets as well as novel compounds with activity against the well-characterized resistance mechanisms, including secondary exon 17 *KIT* mutations and *PDGFRA* p.D842V mutations [22]. PLX9486 has the potential to serve the unmet medical need for selective KIT inhibitors targeting secondary *KIT* exon 17 and 18 mutations. An ongoing clinical trial (NCT02401815) is evaluating its efficacy in GISTs that are resistant to approved TKI. In addition, the unique ability of PLX9486 to inhibit secondary A-loop mutations also makes it an ideal candidate to combine with other TKIs (e.g., sunitinib and PLX3397) with complementary KIT-mutant inhibition profiles that have activities against exon 13 and 14 mutations.

In conclusion, we show that PLX9486 is active in imatinib-resistant GIST both in vitro and in vivo. The compound inhibits cell proliferation and KIT signaling, with anti-tumor activity observed in PDX models. These data warrant further exploration of PLX9486 in clinical trials either as a single agent or in combination with other targeted agents.

Acknowledgements Plexxikon (Berkeley, CA, USA) provided PLX9486 and financial support for the study.

Compliance with ethical standards

Conflict of interest Plexxikon provided PLX9486 and financial support for the study. EAB, BM, GH, JL, MN, GW, CZ and GB are employees of Plexxikon Inc. PS received institutional support from Plexxikon for advisory/consultancy, research funding and travel/accommodation/expenses.

References

1. Nishida T, Blay JY, Hirota S, Kitagawa Y, Kang YK. The standard diagnosis, treatment, and follow-up of gastrointestinal stromal tumors based on guidelines. Gastric Cancer. 2016;19:3–14.
2. Joensuu H, Hohenberger P, Corless CL. Gastrointestinal stromal tumour. Lancet. 2013;382:973–83.
3. Joensuu H, Vehtari A, Riihimäki J, et al. Risk of recurrence of gastrointestinal stromal tumour after surgery: an analysis of pooled population-based cohorts. Lancet Oncol. 2012;13:265–74.
4. Debiec-Rychter M, Sciot R, Le Cesne A, et al. KIT mutations and dose selection for imatinib in patients with advanced gastrointestinal stromal tumours. Eur J Cancer. 2006;42:1093–103.
5. Antonescu CR, Besmer P, Guo T, et al. Acquired resistance to imatinib in gastrointestinal stromal tumor occurs through secondary gene mutation. Clin Cancer Res. 2005;11:4182–90.
6. Demetri GD, van Oosterom AT, Garrett CR, et al. Efficacy and safety of sunitinib in patients with advanced gastrointestinal stromal tumour after failure of imatinib: a randomised controlled trial. Lancet. 2006;368:1329–38.
7. Demetri GD, Reichardt P, Kang YK, et al. GRID study investigators. Efficacy and safety of regorafenib for advanced gastrointestinal stromal tumours after failure of imatinib and sunitinib (GRID): an international, multicentre, randomised, placebo-controlled, phase 3 trial. Lancet. 2013;381:295–302.
8. Heinrich MC, Maki RG, Corless CL, et al. Primary and secondary kinase genotypes correlate with the biological and clinical activity of sunitinib in imatinib-resistant gastrointestinal stromal tumor. J Clin Oncol. 2008;26:5352–9.
9. George S, Wang Q, Heinrich MC, et al. Efficacy and safety of regorafenib in patients with metastatic and/or unresectable GI stromal tumor after failure of imatinib and sunitinib: a multicenter phase II trial. J Clin Oncol. 2012;30:2401–7.
10. Liegl B, Kepten I, Le C, et al. Heterogeneity of kinase inhibitor resistance mechanisms in GIST. J Pathol. 2008;216:64–74.
11. Bollag G. Optimizing kinase inhibitors to treat cancer. Cancer Res. 2016;76 **(abstract IA32)**.
12. Warmuth M, Kim S, Gu X, Xia G, Adrián F. Ba/F3 cells and their use in kinase drug discovery. Curr Opin Oncol. 2007;19:55–60.
13. Van Looy T, Gebreyohannes YK, Wozniak A, et al. Characterization and assessment of the sensitivity and resistance of a newly established human gastrointestinal stromal tumour xenograft model to treatment with tyrosine kinase inhibitors. Clin Sarcoma Res. 2014;4:10.
14. Mullins C, Ricono J, Carson P, et al. A patient derived xenograft (PDX) platform for development of next generation KIT kinase inhibitors in imatinib-resistant gastrointestinal stromal tumors (GIST). Cancer Res. 2014;74(Suppl 19) **(Abstract 1224)**.
15. Gebreyohannes YK, Schöffski P, Van Looy T, et al. Cabozantinib is active against human gastrointestinal stromal tumor xenografts carrying different KIT mutations. Mol Cancer Ther. 2016;15:2845–52.
16. Sciot R, Debiec-Rychter M. GIST under imatinib therapy. Semin Diagn Pathol. 2006;23:84–90.
17. Choi H, Charnsangavej C, Faria SC, et al. Correlation of computed tomography and positron emission tomography in patients with metastatic gastrointestinal stromal tumor treated at a single institution with imatinib mesylate: proposal of new computed tomography response criteria. J Clin Oncol. 2007;25:1753–9.
18. Ran L, Sirota I, Cao Z, et al. Combined inhibition of MAP kinase and KIT signaling synergistically destabilizes ETV1 and suppresses GIST tumor growth. Cancer Discov. 2015;5:304–15.
19. Li F, Huynh H, Li X, et al. FGFR-mediated reactivation of MAPK signaling attenuates antitumor effects of imatinib in gastrointestinal stromal tumors. Cancer Discov. 2015;5:438–51.
20. Gebreyohannes YK, Wozniak A, Zhai ME, et al. Robust activity of avapritinib, potent and highly selective inhibitor of mutated KIT, in patient-derived xenograft models of gastrointestinal stromal tumors. Clin Cancer Res. 2018. https://doi.org/10.1158/1078-0432.CCR-18-1858.
21. Miselli F, Negri T, Gronchi A, et al. Is autophagy rather than apoptosis the regression driver in imatinib-treated gastrointestinal stromal tumors? Transl Oncol. 2008;1:177–86.
22. Bauer S, Joensuu H. Emerging agents for the treatment of advanced, imatinib-resistant gastrointestinal stromal tumors: current status and future directions. Drugs. 2015;75:1323–34.